pH and Particle Structure Effects on Silica Removal by Coagulation

Daphne Hermosilla[†*], Ruth Ordóñez[†], Laura Blanco, Elena de la Fuente and Ángeles Blanco

Department of Chemical Engineering, Universidad Complutense de Madrid, Avda. Complutense, s/n. 28040 Madrid (Spain)

[*]To whom correspondence should be addressed:

Tel.: +34 91 394 4247. Fax: +34 91 394 4243. E-mail: dhermosilla@quim.ucm.es

Abstract

Coagulation is presented as an efficient alternative to reduce the silica content in effluents from recovered-paper mills that are intended to be recycled by a final reverse-osmosis (RO) step. Coagulation pretreatment by several polyaluminum chlorides (PACls) or $FeCl_3$ was optimized prior to the RO process. PACls with low alumina content and high basicity achieved almost a 100% removal of silica at pH 10.5. A good reduction of the silica content was attained without regulating the pH by adding one of these PACls. Silica removal was related to the structure of the produced clots in which cylindrical particles produced higher silica removal. All coagulants removed more than 50% of the chemical oxygen demand (COD).

Keywords: Coagulation, Focused beam reflectance, Paper mill effluent, Reverse osmosis, Silica fouling

Introduction

Reverse osmosis (RO) is the preferred final step when an advanced wastewater treatment is implemented to recycle final effluents in paper mills because it ensures the reduction of conductivity and the total removal of pathogens [1–3]. Effluents from recovered-paper mills usually carry an important content of silica (SiO_2), which causes important scaling and fouling in RO membranes [4], leading to lower water production rates, worse quality of the permeate, unsteady-state operation conditions, and serious physical damage to the membranes themselves [5, 6]. This high silica content mainly comes from sodium silicate, which is added during de-inking processes in order to: (i) stabilize hydrogen peroxide added for bleaching pulp in the pulper; (ii) take advantage of its buffering and saponification properties [7, 8]; (iii) assist the dispersion of ink particles and influence their size [9, 10]; (iv) support ink collection [11]; (v) reduce fiber losses; and (vi) avoid flotation of fillers [12].

Silica may be found either in crystalline form or amorphous state. While crystalline silica addresses a solubility of 5–6mg L^{-1} (25 °C, pH < 9), the solubility of amorphous silica ranges from 120 to 150mg L^{-1} (25 °C, pH < 8.0–8.5) [13]. Amorphous silica is furthermore classified as dissolved (reactive) silica, colloid (non-reactive) silica, and particulate (suspended) silica [6]. The dissolution process of amorphous silica takes

place when silica-oxygen-silica bonds are hydrolyzed forming tetrameric monosilicic acid (H_4SiO_4), the strength of which is weak. The solubility of amorphous silica is mainly affected by temperature (T), pH, and the presence of other ions and organic compounds. The effect of pressure (P) has been demonstrated to be negligible at values up to a few hundred bar at T < 100 °C [14]. Specifically, H_4SiO_4 is generally deionized at a neutral pH value, while, as OH^- concentration increases in the solution, the ionization of silicic acid into $H_3SiO_4^-$ and $H_2SiO_4^{2-}$ (the most predominant species of dissolved silica under alkaline environments) is facilitated [15], therefore, only 10% is ionized at pH 8.5 and 50% is ionized at pH 10.

Dissolved silica interacts with a wide variety of organic and inorganic species, resulting in the formation of complexes that can be deposited on membranes. When Al^{3+} and Fe^{3+} coexist in water feeding the RO system, silica is precipitated even below its saturation point [16]. Al^{3+} and Fe^{3+} contents must be lower than 0.05mg L–1 to work safely [5]. In addition, when the Mg^{2+} content is high and magnesium silicate precipitation must be avoided, the product of silica (expressed as mg SiO_2 L–1) and Mg^{2+} (expressed as mg$CaCO_3$ L^{-1}) contents must be kept below 20 000mg^2L^{-2} when the pH is higher than 7.5 [17]. In addition to silicate precipitation, silica can also foul RO membranes by polymerization [18]. Silica polymerization increases with water hardness, although polymerization is favored at [SiO_2] >300 mg L^{-1} even in the absence of calcium and magnesium [19].

Several technologies have been successfully applied to remove silica from water, namely: (i) those based on increasing the solubility of silica, such as pH and/or T regulation, or the addition of antiscalant products [20, 21]; (ii) addition of chemicals to induce silica coagulation or precipitation; (iii) lime softening [22]; (iv) substitution of antiscalant agents by desupersaturation units, forcing the precipitation of sparingly soluble salts [23], such as calcium carbonate, calcium sulfate, silica, calcium phosphate, and barium sulfate; (v) addition of strong anionic-exchange resins in hydroxide form that assist the removal of silica, which acts as a very weak acid [24, 25]. As the solubility of silica strongly depends on the pH, silica precipitation may be avoided working at pH >10, at which silica solubility increases up to 300–350 mg L^{-1} [13], although the generation of carbonate ions is also favored at this pH value, leading to greater calcium carbonate scaling on RO membranes [26, 27].

Both soluble and colloidal silica can be successfully removed from water by co-precipitation with soluble metals, or by adsorption on freshly formed insoluble hydroxides added to water. For example, the removal of dissolved silica through the formation of $Fe(OH)_3$ has been addressed successfully at pH ≥9.0 after adding NaOH or $Ca(OH)_2$ to a solution containing $Fe_2(SO_4)_3$ [28]. $Mg(OH)_2$ has shown a particularly strong tendency to react with silica [29]. On the other hand, the presence of salts reduces the solubility of amorphous silica, and an alkaline environment favors the formation of silicate ion, which reacts with metal ions forming insoluble silicates [30]. In addition, alumina (Al_2O_3), aluminum chloride, and sulfate salts are also considered excellent adsorbents for dissolved and colloidal silica. Particularly, the amount of Al^{3+} needed to remove colloidal silica was assessed lower than the corresponding quantity to remove dissolved silica at pH 4.1–4.7 [31]. Maximum silica adsorption on Al_2O_3 (≈ 90 %) was achieved at pH 8.0–8.5 [32].

Considering examples from industrial wastewater treatment, 60% silica content has been reported to be removed by $FeCl_3$ coagulation in effluents from two different paper mills [33]. The optimal combination of NaOH with $MgCl_2 \cdot 6H_2O$ and

$ZnSO_4 \cdot 7H_2O$ reduced the silica content in more than 60% from heavy-oil wastewaters [34]. Although these are good examples of how coagulation has been already successfully applied to reduce the silica content in wastewater, very limited research efforts have been made to monitor the coagulation process itself in relation to particle properties in real industrial wastewater [35].

The main objective of this research was to assess the efficiency of different coagulants, including those modified to exhibit high basicity content or containing micropolymers, for removing silica from the final effluent of a recovered-paper mill that is meant to be recycled by a final RO step aiming to reduce freshwater consumption within the mill. Results will be discussed considering coagulation mechanisms, properties of the coagulants, and structure of the formed coagula.

2. Materials and Methods

Samples were taken from the effluent of a 100% recovered-paper mill located in Madrid, Spain. This wastewater is previously treated by aerobic digestion and dissolved air flotation to degrade organic matter and remove suspended solids, respectively, before been dumped into the municipal wastewater treatment plant. Samples were first filtered through 150 µm filters and then characterized before been stored at ± 4 °C for four days maximum. Results are summarized in Tab. 1. All analyses were performed following the Standard Methods for Examination of Water and Wastewater [36]. In short, samples were additionally filtered through 1 µm filters before measuring alkalinity, hardness, chloride, iron, calcium, and aluminum contents, and through 0.45 µm filters before measuring soluble chemical oxygen demand (COD), sulfate, and silica (as SiO_2). Particularly, reactive SiO_2 to molybdosilicic acid ($H_4Mo_{12}O_{40}Si$) was measured by flow injection analysis (FIA) and photometric detection, as described in the method DIN EN ISO 16264: 2004/2005, using an FIA compact device (Medizin- und Labortechnik Engineering GmbH, Dresden, Germany).

One iron salt ($FeCl_3$) and five polyaluminum chlorides (PACl1, PACl2, PACl3, PACl4, and PACl5) from Kemira Ibérica S.A. (Spain) were tested as coagulants. Tab. 2 summarizes their main properties. All coagulants were delivered as a liquid suspension and diluted to the desired concentration adding tap water the same day they were used.

Polyaluminum coagulants are typically characterized by their basicity, which is related to the quantity of Al-polymeric species formed in water during coagulation. Basicity was calculated as follows [37]:

$$Basicity\,(\%) = 100 \cdot \left(\frac{1}{3} \cdot \frac{[OH^-]}{[Al_T]} \right) \quad (1)$$

where $[OH^-]$ and $[Al_T]$ designate the concentration of base and aluminum, respectively, that are present in the chemical formulation of the coagulant.

The optimal dosage of each coagulant was determined by monitoring the process with a commercially available non-imaging scanning laser microscope or focused beam reflectance measurement device (FBRM) [38], manufactured by Auto-Chem, Mettler Toledo (Seattle, WA, USA). The FBRM instrument operates by scanning the particles in suspension with a laser beam at a focal point that describes a circular path. When a particle intercepts this path, the time duration of the backscattered light from this particle is measured and multiplied by the velocity of the scanning laser, which is a

known characteristic of the device, resulting in a characteristic dimensional measurement of the geometry of the particle, namely the chord length. Thousands of chord length measurements (i.e., number of counts) are collected per second, producing a histogram in which the number of the observed counts is sorted in several chord length bins over the range of 0.5–1000 or 2000 lm [38]. All the experiments with the FBRM were programmed to obtain a chord length distribution every 5 s, so that enough particles are detected to get a good representative distribution of the population.

Table 1. Characterization of the paper mill effluent.

Parameter	Units	Mean	Std. dev.
pH	[–]	8.6	0.3
Conductivity	[mS cm^{-1}]	3.1	0.4
Total suspended solids (TSS)	[mg L^{-1}]	145	74
Soluble COD	[mg L^{-1}]	505	174
Alkalinity	[mg_{CaCO_3} L^{-1}]	400	75
Hardness	[mg_{CaCO_3} L^{-1}]	150	2
Turbidity	[NTU]	158	21
SO_4^{2-}	[mg L^{-1}]	582	122
Cl^-	[mg L^{-1}]	110	28
Si	[mg_{SiO_2} L^{-1}]	185	31
Fe_{total}	[mg L^{-1}]	0.9	0.1
Ca	[mg_{CaCO_3} L^{-1}]	138	25
Al^{3+}	[mg L^{-1}]	0.09	0.06

Table 2. Chemical specifications of the coagulants.

Coagulant	Concentration [wt-%]	Al_2O_3 [%]	Basicity [%]	Other
$FeCl_3$	39–47	–	–	–
PACl1	–	17.0 ± 0.5	42 ± 2	–
PACl2	–	17.0 ± 0.5	43 ± 5	High molecular weight
PACl3	–	9.5 ± 1.0	70 ± 5	Contains micropolymers
PACl4	–	9.7 ± 0.3	85 ± 10	–
PACl5	–	9.7 ± 0.3	85 ± 10	Contains micropolymers

Coagulant (100 mg L^{-1}) was added to water samples of 0.15 L every 10 s under stirring at 270 rpm. Each dosage optimization experiment finished when water was saturated with the coagulant reaching a constant value for both, the mean chord length (MCL) and the total number of counts (TNC) per second. Since pH affects the coagulation process, experiments were run at three different initial pH values: 5.5 (acidic), 8.6 (typical for the wastewater sample, Tab. 1; no pH regulation was required),

and 10.5 (basified); 0.1M HCl was used to adjust the pH to 5.5 and 1M NaOH was added to reach pH 10.5. The flow diagram of the installation used to perform these coagulation trials is presented in Fig. 1.

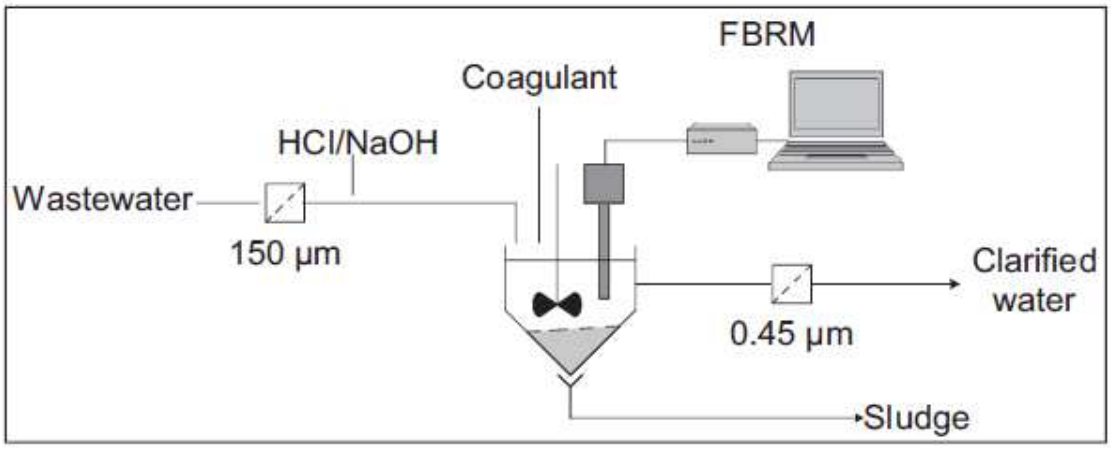

Figure 1. Flow diagram of the installation used to perform the coagulation trials

Each coagulation trial was repeated three times. After performing every coagulation treatment, clarified water was timely filtered for measuring conductivity, soluble COD, silica, chloride, iron, and aluminum contents, as described above. The type and size of coagulated particles were determined by analyzing images taken by an optical microscope (Olympus BX41). Scanning electron microscopy-energy dispersive X-ray spectroscopy (SEM-EDS) was applied to determine the atomic composition of the aggregates formed by the coagulants using a Jeol JSM-6400 scanning electron microscope.

Sedimentation rates were calculated for the most efficient treatments. After addition of the coagulant to a jar containing 0.5 L of water, the sample was stirred at 180 rpm for 5 min before slowing down the agitation rate to 45 rpm for 10 min. Finally, the solution was allowed to settle for 120 min, along which the height of the sediment was periodically measured.

Analysis of variance was performed to test the effects of pH and coagulant type on the removal efficiency of silica content and COD. Tukey's test was used for all pairwise comparisons of mean values ($P < 0.05$). Nonlinear regression was applied to explain the relationship between some measured results.

3 Results and Discussion

The optimal dosage of each coagulant at every tested pH value was determined as the minimum required coagulant addition that maximized the TNC per second and the MCL determined by the FBRM probe (Figs. 2–4). In general, no effect was detected before reaching a certain dosage threshold, and a steady state was achieved when no cumulative effect was observed after increasing the dosage.

At the beginning of the experiments, dissolved and colloidal material (DCM) might have not been detected because particles were smaller than 1 lm, which is the detection size limit of the FBRM. DCM destabilized as more coagulant was added, thus, the incipient formation of aggregates was detected by FBRM as an increase of the TNC [39]. The size of these aggregates usually increases as well along the coagulation trial

resulting in a corresponding increase of the MCL. The main source of DCM in the mill's wastewater is recovered paper, although some chemical additives used during the manufacturing process may also contribute. Stickies, salts and organic compounds released during pulping, dispersing, and bleaching, are substances that may be included within this fraction [40].

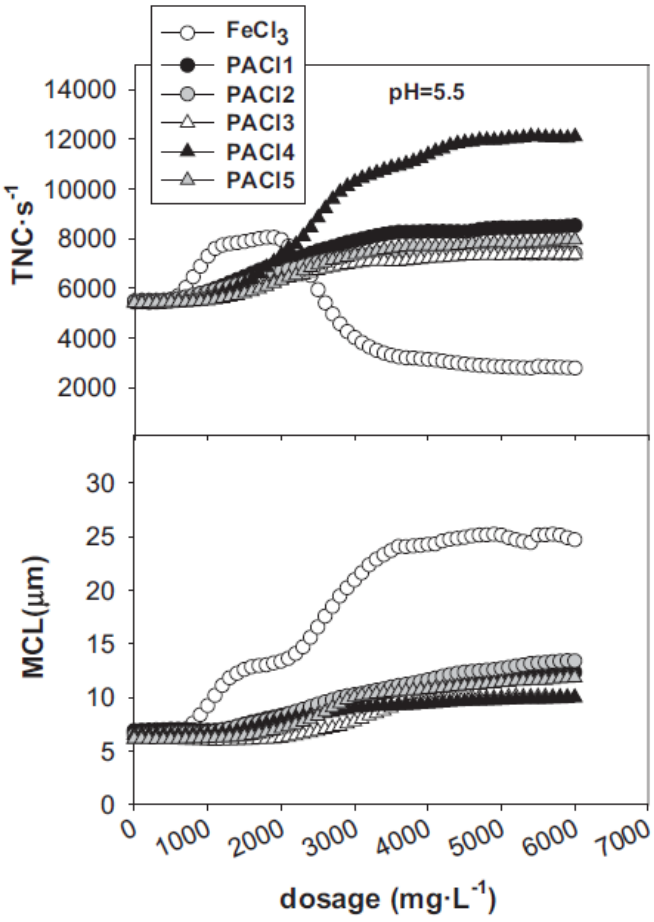

Figure 2. Evolution of the total number of counts (TNC) per second and mean chord length (MCL) as the coagulant dosage increases at pH 5.5.

Particularly, the addition of $FeCl_3$ was apparently able to generate bigger coagula than PACls under all tested pH conditions, as detected by FBRM (Figs. 2–4). The optimal dosage of $FeCl_3$ maximizing TNC and MCL increased from acid to basic condition of the solution from 1500 to about 2500 mg L^{-1}. In general, the formation of aggregates was detected at lower concentration thresholds than in the case of low-basicity PACls. The observed decrease in the TNC in the presence of $FeCl_3$ at pH 5.5 (Fig. 2) denotes that doses higher than 2500 mg L–1 cause the predominant coagulation of particles and aggregates larger than 1 µm.

In addition, both low-basicity PACls (PACl1 and PACl2, Tab. 2) exhibited some similar performance patterns to $FeCl_3$ trials, i.e., the TNC progressively increased to a maximum when a higher coagulant dose was added at any pH value of the solution (Figs. 2–4), and MCL increased at higher coagulant doses at pH 5.5 (Fig. 2) and 10.5 (Fig. 4). In addition, MCL decreased to a minimum value more pronouncedly than in the case of $FeCl_3$ when the pH was not regulated (pH 8.6, Fig. 3), even though the TNC began to increase. At this point, the coagulant dosage was lower than 2000 mg L–1 for

all these three coagulants ($FeCl_3$ and both low-basicity PACls). The coagulation of the smallest DCM particles that were not initially detected by the FBRM (< 1 lm) may explain why MCL decreases as the TNC increases at a dosage below 2000 mg L–1. The addition of a higher dose of these coagulants resulted in the generation of enough larger particles to make MCL finally increase. In general, the coagulant dosage at which MCL remained more or less constant was higher for the trials performed at higher pH values (Figs. 2–4).

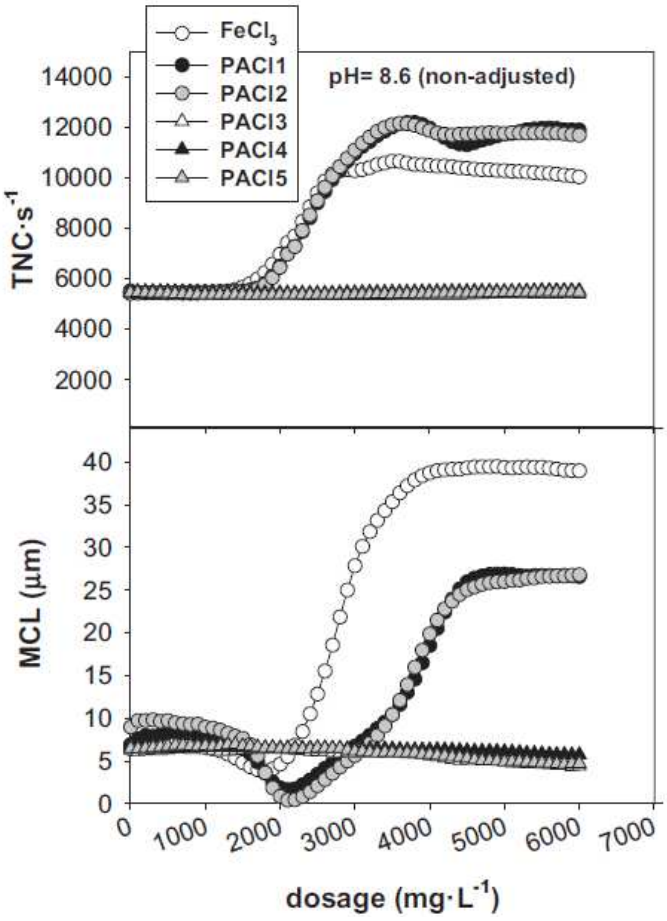

Figure 3. Evolution of the TNC per second and MCL as the coagulant dosage increases without pH regulation (pH 8.6).

In contrast, the behavior of high-basicity PACls (PACl3, PACl4, and PACl5) was totally different from that of $FeCl_3$ and low-basicity PACls (PACl1 and PACl2) under alkaline conditions. MCL kept constant and TNC decreased very slightly, indicating that these coagulants did not induce a significant amount of measurable particle aggregation at these pH values. Changes in the morphology of suspended particles were, however, observed under the microscope. Coagulation phenomena took place despite the FBRM did not properly detect what occurred. Particles were aggregated linearly, generating cylindrical coagula with the same diameter than the original particles, but much longer (Fig. 5). This kind of particle aggregation slightly diminished the TNC at an increasing coagulant dosage but the shape of the aggregates did not make the MCL increase because the probability that the focal point of the FBRM probe covered these particles lengthwise was very low.

The decrease of the TNC due to the aggregation of measurable particles might have been compensated by the increase of the TNC caused by the coagulation of

particles smaller than 1 µm, thus resulting in no significant change of the TNC when more coagulant was added at pH 8.6. Coagulation of DCM <1µm should have been predominant at pH 5.5, therefore producing an increase of the TNC and generating larger coagulated particles than the current mean coagula size which in turn results in higher MCLs. Finally, the aggregation of coagulated particles larger than 1 µm was predominant at pH 10.5, so the TNC correspondingly decreased.

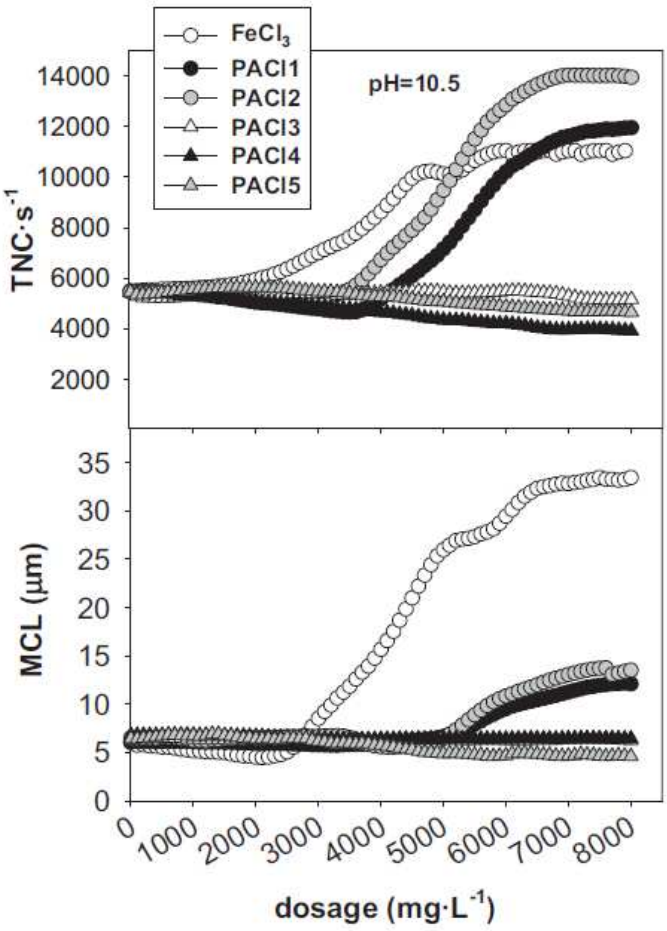

Figure 4. Evolution of the TNC per second and MCL as the coagulant dosage increases at pH 10.5.

As it was previously demonstrated, the addition of $FeCl_3$ apparently generated bigger coagula than PACls at all tested pH values (Figs. 2–4). Photographs taken by optical microscopy indicated that $FeCl_3$ really produced larger and more spherical aggregates than PACls (Fig. 5). These results agree with previous research reporting that $FeCl_3$ and $TiCl_4$ produced larger and more spherical aggregates than aluminum salts (aluminum and one PACl) [41]. They also flocculated faster, i.e., while 5 min were enough to perform an optimal coagulation by $FeCl_3$, 15 min were required by the tested PACl. As a result, high-basicity PACls produced longer and more defined structured aggregates than low-basicity ones (Fig. 5), and these aggregates were able to remove a significantly higher silica content (Tab. 3).

The optimal doses of each coagulant at different pH conditions were considered as the non-saturating ones producing maximum TNC (Figs. 2–4). At a constant TNC, MCL may still increase due to the aggregation of smaller particles that have already been formed, but the coagulation treatment would not perform further significant removal of silica and COD. When the TNC was constant or slightly decreasing

regardless increasing the coagulant dosage (e.g., PACls at pH 8.6 and 10.5), the maximum dosage added to the sample was chosen to assess the efficiency of the treatment. For the same coagulant, a higher amount of silica was removed with a higher initial pH value of the solution (Tab. 3) but the required dosage of the coagulant was also much higher. In short, the best efficiencies (> 95 %) in removing the dissolved silica content were obtained after adding high doses of high-basicity PACls at pH 10.5.

Table 3. Coagulation treatment efficiency in terms of dissolved silica and COD removals, and conductivity. Letters (a–e) label heterogeneous groups of mean values by Tukey's test ($P < 0.05$; $n = 3$), as the interaction of factors resulted significant.

Coagulant	pH	Optimal dosage [mg L^{-1}]	SiO_2 [% removal]		COD [% removal]		Conductivity [mS cm^{-1}]	
			Mean	Std. dev.	Mean	Std. dev.	Mean	Std. dev.
$FeCl_3$	5.5	2000	17 ^{e}	2	77 ^{b,c}	3	4.75	0.31
	8.6	3000	25 ^{d,e}	3	87 ^{a}	3	4.09	1.02
	10.5	6000	27 ^{d,e}	5	85 ^{a,b}	1	6.49	0.91
PACl1	5.5	3500	32 ^{d,e}	1	64 ^{b,c,d}	6	4.20	0.76
	8.6	4000	30 ^{d,e}	3	76 ^{b,c}	1	3.93	0.98
	10.5	7000	57 ^{b,c}	4	76 ^{a,b,c}	8	6.16	1.62
PACl2	5.5	3000	41 ^{c,d}	4	63 ^{c,d}	1	4.69	1.65
	8.6	4000	38 ^{c,d}	7	75 ^{a,b,c}	8	3.99	1.17
	10.5	7000	65 ^{b}	1	83 ^{a,b}	6	5.16	0.39
PACl3	5.5	4500	25 ^{c,d,e}	6	72 ^{a,b,c}	7	4.81	0.33
	8.6	6000	67 ^{b}	7	58 ^{c,d}	1	4.35	0.23
	10.5	8000	96 ^{a}	1	56 ^{c,d}	5	5.09	0.06
PACl4	5.5	4500	28 ^{d,e}	1	78 ^{b,c}	1	3.98	0.95
	8.6	6000	54 ^{b,c}	6	62 ^{c,d}	2	4.65	0.36
	10.5	8000	97 ^{a}	1	53 ^{d}	1	4.95	0.65
PACl5	5.5	4000	25 ^{d,e}	5	78 ^{b,c}	1	4.01	0.78
	8.6	6000	74 ^{b}	5	58 ^{c,d}	2	4.49	0.33
	10.5	8000	96 ^{a}	1	64 ^{b,c,d}	5	5.30	0.21

Depending on the pH and the concentration of aluminum and iron in the solution, two primary coagulation mechanisms can be defined [42]: (i) adsorption of cationic-charged species onto anionic particles, neutralizing its charge and enabling their aggregation, and (ii) enmeshment or sweeping of colloids in $Al(OH)_3$ or $Fe(OH)_3$ precipitates.

PACls hydrolyze when they are added to water, which implies the generation of monomers (Al^{3+}, $Al(OH)^{2+}$), dimers ($Al_2(OH)_2(H_2O)_8$ $^{4+}$), and polymers ($Al_6(OH)_{12}$ $^{6+}$, $Al_{13}O_4(OH)_{24}(H_2O)_{12}$ $^{+7}$). As the pH increases, the amount of these cationic species decreases, and other anionic species appear, such as $Al(OH)_4^-$. The first coagulation mechanism will be active as soon as these cationic species are present in the solution. For the same coagulant dosage, the proportion of these high-valence species increases if

the basicity of the added PACl is higher. Therefore, chemicals with basicity values of >70% (PACl3, PACl4, and PACl5) produce polymeric species with a high cationic charge, among which $Al_{13}O_4(OH)_{24}(H2O)_{12}^{+7}$ (also known as Al_{13}^{7+}) has been reported to be an especially predominant species [37]. Al_{13}^{7+} particles form aggregates whose size and structure depend on its surface charge which is also pH-dependent. While the charge of the aggregates is high at pH4.5 and they exhibit an open structure, the surface charge is lower at higher pH values, driving the structure denser and affecting the performance of coagulation [43]. As a result, the production of well-defined cylindrical coagula was observed (Fig. 5).

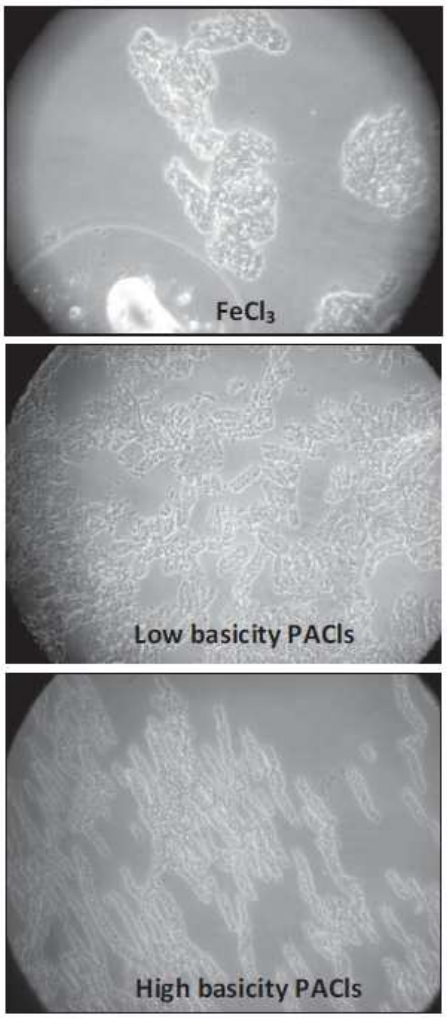

Figure 5. Optical microscope images (20×) of particles formed after adding different types of coagulant at alkaline pH.

In addition, the presence of cationic species in the solution also decreases as the pH increases, which implies that a higher amount of coagulant is required to reach optimum coagulation results (Figs. 2–4). On the other hand, the coagulant concentration added to the solution determines the extent of the second coagulation mechanism mentioned above, so the enmeshment of the colloids will be predominant at higher ratios of $Al(OH)_{3(am)}$ (a solid-amorphous state of the coagulant) to ionized species contents [44]. At pH values ranging from 2.5 to 7.5, silica is present in the solution as SiH_4 species, which do not have ionic charge and are unstable in aqueous solution. At a pH value >7.5, the OH^- concentration increases and facilitates ionization of silicic acid ($H_4SiO_4^0$) into $H_3SiO_4^-$ and $H_2SiO_4^{2-}$ [15]. Furthermore, diverse polymeric species of

silica may be present in the solution (e.g., $Si_2O_3(OH)_4^{2-}$ and $Si_3O_5(OH)_5^{3-}$), and, moreover, polymerization is thought to be catalyzed by hydroxyl anions as well, i.e., it is a very fast process at neutral or slightly alkaline pH values, whereas it is retarded under acid environments [45]. As a consequence of these ionization and polymerization processes, a higher amount of silica may be removed by higher-basicity PACls under basic condition, even more when they contain micropolymers.

On the other hand, the behavior of $FeCl_3$ is very different. When $FeCl_3$ is added to water at natural bicarbonate alkalinity, $Fe(OH)_3$ precipitate is generated and coexists with other hydrated species like Fe^{3+}, $Fe(OH)^{2+}$, and $Fe(OH)^{2+}$, although the concentration of these cationic species is reduced when the pH is >8.0 [44].

In order to reduce scaling potential hazard, the concentration of silica in feed water must be reduced below its saturation limit (≈ 120mg L^{-1}), thus membranes could work at a recovery rate higher than 85% without problems due to silica precipitation. The coagulant doses required to achieve the best silica removal are too high to be feasible at industrial scale. Therefore, additional experiments were performed at pH values of 8.6 and 10.5 using lower doses of high-basicity PACls

(500–2500 mg L^{-1}) aiming to assess if good silica reductions could be achieved as well (Fig. 6). These experiments also enabled the performance of further comparisons among coagulation efficiencies at different dosages.

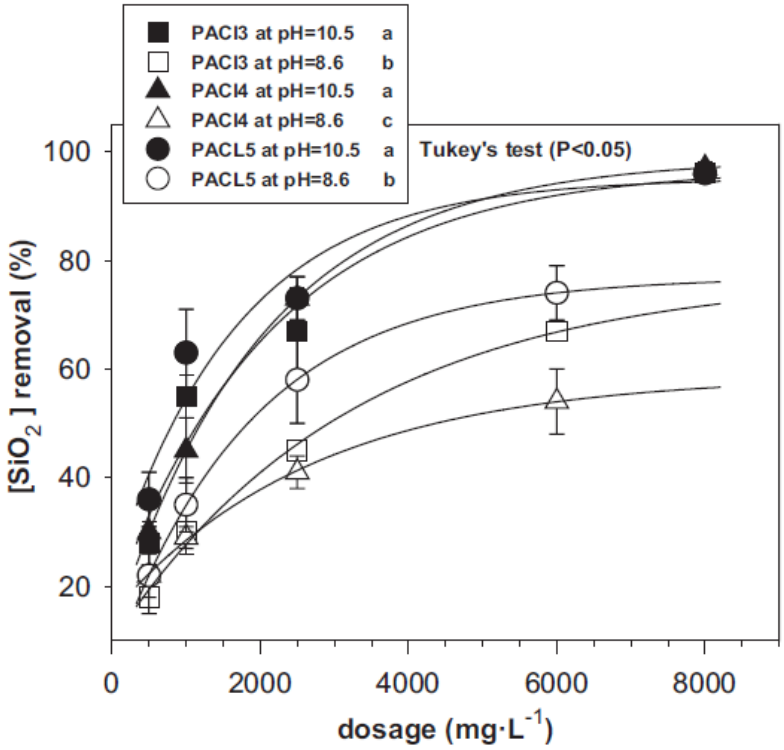

Figure 6. Silica removal using different doses of high-basicity PACls (> 70 %) at basic pH (letters label homogeneous groups among maximum silica content removal values by Tukey's test; $P < 0.05$; n = 3).

As a result, the silica content was reduced up to 65–75% using 2500 mg L^{-1} of these high-basicity PACls at pH 10.5 (Fig. 6), thus ensuring that the RO system may work safely if a recovery rate higher than 50% is pretended. The main drawback of performing these coagulation treatments increasing the pH value of the solution is that the conductivity also increases (Tab. 3). Current legislation of the Region of Madrid sets

a maximum limit of 7.5mS cm^{-1} for the conductivity of industrial effluents that are going to be discharged into municipal water lines [46], a consideration that has to be also taken into account when setting the recovery rate of RO units in this case.

If high-basicity PACls are added at the same lower concentrations, but without regulating the pH in the solution, thus avoiding the increase of conductivity, a 60% silica content was removed when adding 2500 mg L^{-1} of PACl5, while PACl3 and PACl4 removed only about 40% at this dosage (Fig. 6). These results are, however better than the best efficiencies achieved by even higher doses of low-basicity PACls and $FeCl_3$ (3000–4000 mg L^{-1}; Tab. 3). Coagulated particles were analyzed by SEM-EDX, with their main components found as aluminum, oxygen, and silica (Tab. 4). The percentage of the silica content was slightly higher in the particles formed using PACl5.

Table 4. Atomic composition (SEM-EDX) of the coagulated particles formed using high-basicity PACls.

Element	Atomic composition [%]		
	PACl3	PACl4	PACl5
O	55	58	50
Al	35	30	36
Si	8	10	12
Cl	1	1	1
Ca	1	1	1

The results clearly indicated that a similar dosage of high-basicity PACls significantly removes more silica than low-basicity ones at under basic pH conditions (Tab. 3). The size and structure of the aggregates is different by the effect which the pH exerts on its surface charge, affecting the performance of coagulation [43]. In addition, the presence of cationic species is lower at higher pH values. As a consequence of a higher presence of polymerized species, the removal of silica was improved using high-basicity coagulants, whether by increasing its dosage without modifying the pH or by increasing the pH value of the solution while keeping the same coagulant dosage (Fig. 6).

The final objective of reaching high silica removal results must be balanced with a good sedimentation velocity, which is related to the area of the clarifier needed to separate the slurry from the clarified water. Sedimentation capacity was also measured for PACl3, PACl4, and PACl5 after coagulating the samples with 2500 mg L^{-1} of each product at pH 8.6. The sediment compacted more than 300mL after 15 min (Fig. 7), which is considered as a high sedimentation velocity [47]. Most of the sediment was close to be totally compacted after 1 h.

More than 50% of the COD was removed by all considered coagulants at all tested pH values (Tab. 3). In general, a significant significant higher removal of the COD was achieved when the formed aggregates were more spherical (Fig. 5), and, in particular, when a lower silica content was removed from the solution within the trials performed using high-basicity PACls (Fig. 8). Higher pH values enabled higher doses of these coagulants to achieve the highest reductions of silica content despite pulling down the removal of COD. Good reductions of both silica content and COD could be,

however, achieved together in some cases.

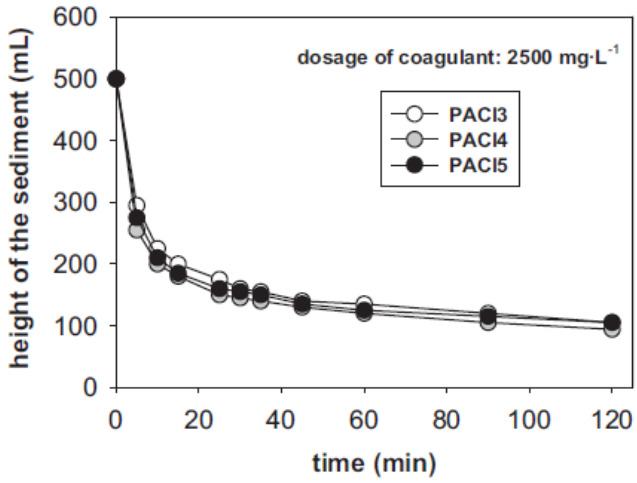

Figure 7. Sedimentation velocity after adding 2500mgL^{-1} of high-basicity PACls.

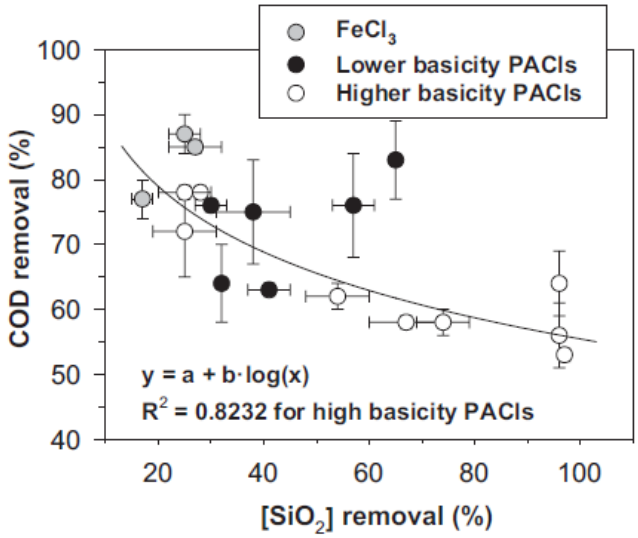

Figure 8. COD and SiO_2 removal for high-basicity PACls.

4. Conclusions

pH modification to increase the solubility of silica is not recommended whenever there is a risk of carbonate scaling. In such case, coagulation represents a feasible alternative for removing the silica content. The efficiency of the selected coagulants on the reduction of silica content was related to the structure of the formed particles rather than to the size of the aggregates or to DCM destabilization to form larger coagula. Cylindrical particle morphologies were identified to be formed in the cases achieving higher silica removal efficiencies. The use of $FeCl_3$ induced the formation of the largest and most spherical aggregates, resulting in the achievement of the highest COD removal and the lowest silica removal values (< 30 %).

A high silica removal efficiency (> 90 %) was obtained by performing coagulation treatments with high-basicity PACls (PACl3, PACl4, and PACl5) increasing the pH of the final paper mill effluent up to 10.5, although the required

coagulant doses were very high. Furthermore, the conductivity of the solution increased as well, which represents another potential limitation for water recovery from RO systems.

About 60% reduction of the silica content of wastewater was achieved using 2500 mg L^{-1} of one high-basicity PACl without regulating the pH. This coagulant is characterized by its high basicity value (85 %) and its content of micropolymers. All coagulants achieved reductions in COD > 50% at all tested pH values, although high-basicity PACls tended to decrease their COD removal efficiency at higher pH and dosage, achieving in contrast an almost total removal of the silica content

Acknowledgment

This research was developed in the framework of the following projects: "PROLIPAPEL" (P2009/AMB-1480), funded by the Regional Government of Madrid (Comunidad Autónoma de Madrid), Spain, "AGUA Y ENERGÍA" (CTM2008-06886-C02- 01), funded by the Ministry of Science and Innovation of Spain (Ministerio de Ciencia e Innovación), and "AQUAFIT- 4USE" (211534), funded by the European Commission. We would like to thank Kemira Ibérica for supplying the coagulants.

The authors have declared no conflict of interest.

Symbols used

COD: [mg L^{-1}] chemical oxygen demand

MCL: [µm] mean chord length

T: [°C] temperature

Abbreviations

DCM: dissolved and colloidal material

FBRM: focused beam reflectance measurement

FIA: flow injection analysis

PACls: polyaluminum chlorides

RO: reverse osmosis

SEM-EDS: scanning electron microscopy-energy dispersive X-ray spectroscopy

TNC: total number of counts

References

[1] J. A. Cotruvo, G. F. Craun, N. Hearne, Providing Safe Drinking Water in Small Systems: Technology, Operations and Economics, CRC Press, Boca Raton, FL 1999.

[2] Low-Pressure Membrane Filtration for Pathogen Removal: Application, Implementation and Regulatory Issues (EPA 815- C-01-001), Environmental Protection Agency, Washington, DC 2001.

[3] A. Bennet, Filtr. Sep. 2008, 45 (1), 14.

[4] R. Sheikholeslami, S. Tan, Desalination 1999, 126 (1–3), 280.

[5] M. Al-Ahmad, F. A. Abdul, A. Mutiri, A. Ubaisy, Desalination 2000, 132 (1–3), 173.

[6] C. J. Gabelich, W. R. Chen, T. I. Yun, B. M. Coffey, I. H. Suffet, Desalination 2005, 180 (1–3), 307.

[7] L. Ferguson, Tappi J. 1992, 75 (7), 75.

[8] L. Ferguson, Tappi J. 1992, 75 (8), 49.

[9] T. Ali, F. McLellan, J. Adiwinata, M. May, T. Evans, J. Pulp Pap. Sci. 1994, 20 (1), J3.

[10] M. Mahagaonkar, P. Banham, K. Stack, Prog. Pap. Recycl. 1997, 6, 50.

[11] A. Santos, B. Carre, A. Roring, in Proc. of Recycling Symp., Tappi Press, Atlanta 1996.

[12] I. Mathur, in Proc. of Recycling Symp., Tappi Press, Atlanta 1994.

[13] R. K. Iler, The Chemistry of Silica. Solubility, Polymerization, Colloid and Surface Properties and Biochemistry, Wiley-Interscience, New York 1979.

[14] R. Sheikholeslami, S. Zhou, Desalination 2000, 132 (1–3), 337.

[15] T. S. Huuha, T. A. Kurniawan, M. E. T. Sillanpää, Chem. Eng. J. 2010, 158, 584.

[16] M. Luo, Z. Wang, Desalination 2001, 141 (1), 15.

[17] P. F. Weng, Desalination 1995, 103 (1–2), 59.

[18] M. Dietzel, Geochim. Cosmochim. Acta 2000, 64 (19), 3275.

[19] T. Koo, Y. J. Lee, R. Sheikholeslami, Desalination 2001, 139 (1–3), 43.

[20] C. W. Smith, Pilot Test Results Utilizing Polymeric Dispersants for Control of Silica, Water Soluble Polymers: Solution Properties and Application (Ed.: Z. Amjad), Plenum Press, New York 1998.

[21] M. J. White, J. L. Masbate, Ultrapure Water 2001, 18 (7), 56.

[22] I. S. Al-Mutaz, I. A. Al-Anezi, Conf. on Water Resources and Arid Environment, Riyadh, December 2004.

[23] I. Bremere, M. Kennedy, P. Michel, R. van Emmerik, G.-J.Witkamp, J. Schippers, Desalination 1999, 124 (1–3), 51.

[24] E. Zaganiaris, S. Doulut, L. Morino, React. Polym. 1992, 17 (1), 15.

[25] A. M. Ben Sik Ali, B. Hamrouni, S. Bouguecha, M. Dhahbi, Desalination 2004, 167, 273.

[26] Reverse Osmosis Membranes, Technical Manual, Filmtec Corp., Dow Chemical Company, Midland, MI 2005.

[27] T. Asano, F. Burtun, H. Leverenz, R. Tsuchihashi, G. Tchobanoglous, Water Reuse: Issues, Technologies and Applications, 1st ed., Metcalf and Eddy, McGraw Hill, Palo Alto, CA 2007.

[28] S. D. Faust, O. M. Aly, in Chemistry of Water Treatment (Eds: S. D. Faust, O. M.

Aly), Butterworth Publishers, Boston, MA 1983.

[29] R. Y. Ning, Desalination 2002, 151 (1), 67.

[30] R. Sheikholeslami, I. S. Al-Mutaz, T. Koo, A. Young, Desalination 2001, 139 (1–3), 83.

[31] H. Roque, Chemical Water Treatment: Principles and Practice, VHC Publishers Inc., New York 1996.

[32] W. Bouguerra, M. Ben Sik Ali, B. Hamrouni, M. Dhahbi, Desalination 2007, 206 (1–3), 141.

[33] E. El-Bestawy, I. El-Sokkary, H. Hussein, A. F. Abu Keela, J. Ind. Microbiol. Biotechnol. 2008, 35 (11), 1517.

[34] Y. B. Zeng, C. Z. Yang, W.H. Pu, X. L. Zhang, Desalination 2007, 216 (1–3), 147.

[35] M. R. Chang, D. J. Lee, Y. J. Lai, J. Environ. Manage. 2007, 85 (4), 1009.

[36] A. E. Eaton, L. S. Clesceri, E. W. Rice, A. E. Greenberg, M. A. H. Franson, Standard Methods for the Examination of Water and Wastewater, American Public Health Association (APHA), American Water Works Association (AWWA), Water Environment Federation (WEF), USA 2005.

[37] D. J. Pernitsky, J. K. Edzwald, Water Supply 2006, 55 (2), 121.

[38] A. Blanco, E. Fuente, C. Negro, J. Tijero, Can. J. Chem. Eng. 2002, 80 (4), 734.

[39] R. Miranda, A. Blanco, E. Fuente, C. Negro, Sep. Sci. Technol. 2008, 43 (14), 3732.

[40] J. Brun, T. Delagoutte, B. Carre, Prog. Pap. Recycl. 2007, 17 (1), 12.

[41] S.-H. Kim, J.-S. Yoon, S. Lee, Desalin. Water Treat. 2009, 10 (1–3), 95.

[42] W. Stumm, C. R. O'Melia, J. AWWA 1968, 60 (5), 514.

[43] A. Torra, F. Valero, J. L. Bisbal, J. F. Tous, Tecnología del Agua 1998, 177 (18), 58.

[44] C. J. Gabelich, T. I. Yun, B. M. Coffey, I. H. Suffet, Desalination 2002, 150 (1), 15.

[45] N. D. Tzoupanos, A. I. Zouboulis, C. A. Tsoleridis, Colloids Surf., A 2009, 342 (1–3), 30.

[46] Law 10/1993, October 26 (Madrid Region Regulation, Spain), Liquid Effluents Dumping to the Integral Sanitation System, Madrid 1993.

[47] C. Allegre, M. Maisseu, F. Charbit, P. Moulin, J. Hazard. Mater. 2004, 116 (1–2), 57.